A new use for modified sugarcane bagasse containing adsorbed Co^{2+} and Cr^{3+}: Catalytic oxidation of terpenes

Anderson Gabriel Marques da Silva, Thenner Silva Rodrigues, Leandro Vinícius Alves Gurgel, Patrícia Aparecida de Assis, Laurent Frédéric Gil[*], Patricia Alejandra Robles-Dutenhefner[*]

Departamento de Química, Instituto de Ciências Exatas e Biológicas, Universidade Federal de Ouro Preto, Campus Universitário Morro do Cruzeiro, 35400-000 Ouro Preto, Minas Gerais, Brazil

A B S T R A C T

This study describes the applicability of two chemically modified sugarcane bagasses containing either adsorbed Co^{2+} or Cr^{3+} ions as heterogeneous catalysts for the autooxidation of monoterpenes. The main objective was to investigate new uses for these adsorbent materials which had been previously employed for treatment of aqueous solutions or effluents containing metals such as Co^{2+} and Cr^{3+}. The adsorption efficiency of Co^{2+} and Cr^{3+} on SCB2 and EB was evaluated by adsorption isotherms and other techniques such as XRD, ICP-AES and TGA. Catalytic activity of the four new catalysts, SCB2-Co, SCB2-Cr, EB-Co, and EB-Cr, were assessed in the oxidation reaction of β-citronellol(**1**), (+)-limonene(**2**), and (−)-β-pinene(**3**) in a free solvent system. Results obtained demonstrated that these materials were promising catalysts for the oxidation of monoterpenes. Reactant conversion ranged from 49 to 78% as determined by GC analysis and a combined selectivity up to 59% for the oxidation products was achieved.

© 2013 Elsevier B.V. All rights reserved.

1. Introduction

In recent years, the use of lignocellulosic materials as solid supports for the adsorption of metallic cations has received much attention due to the low costs associated with these promising alternative materials (Gurgel et al., 2008a; Sud et al., 2008). Thenceforward, various research groups have developed adsorption materials based on lignocellulosic matrices as solid supports with good chemical affinity for metallic cations. Noteworthy is the fact that amongst the biomass sources available, those originating from agricultural residues such as sugarcane bagasse, wood bark, and wood sawdust have been the most intensively investigated for the development of new adsorbent materials (Ajmal et al., 1998; Gurgel et al., 2008b; Karnitz et al., 2009; Naiya et al., 2009; Pereira et al., 2009; Sud et al., 2008; Yu et al., 2008). In the Brazilian scenario, the use of agricultural residues for novel applications is a particularly attractive and promising source of new materials, given the continually growing investments in recent years by local industry in the production of renewable fuels. According to the Brazilian Ministry of Agriculture, the sugarcane harvest in the 2011/2012 season is expected to reach 571.4 million tons, which will generate about 142.9 million tons of bagasse and 116.6 million tons of straw (CONAB, 2011). Or in other words, one ton of sugarcane produces about 250 kg of bagasse and 204 kg of straw with an estimated moisture content of 50%, and thus highlighting the potential of bagasse derivatives for other industrial applications.

Sugarcane bagasse is mainly composed by 40–50% cellulose, 25–30% polyoses, and 20–25% lignin (Karnitz et al., 2007). The chemical structures of such macromolecules are endowed with hydroxyl groups that can be transformed by modifying agents to incorporate certain functional groups able to adsorb metallic cations with high selectivity. One example of a compound that can be "grafted" into the sugarcane bagasse structure is ethylene-diaminetetraacetic dianhydride (EDTAD). In this case, amine and carboxylic acid functions are released producing a very efficient complexing substructure into the lignocellulosic matrix for metal adsorption (Karnitz et al., 2009). Other agents such as succinic, maleic or phthalic anhydrides can be used to modify the surface of sugarcane bagasse through an esterification reaction resulting in a surface containing carboxylic acid functional groups (—COOH). This kind of functionalization clearly increases the adsorption capacity of the lignocellulosic materials, which has been demonstrated in the literature (Karnitz et al., 2007; Liu et al., 2007, 2008; Naiya et al., 2009; Srivastava et al., 2006; Sud et al., 2008; Sun et al., 2003; Xiao et al., 2001).

* Corresponding authors. Tel.: +55 31 3559 1229/31 3559 1717;
fax: +55 31 3559 1707.
  E-mail addresses: laurent@iceb.ufop.br (L.F. Gil),
pard@iceb.ufop.br (P.A. Robles-Dutenhefner).

Modified sugarcane bagasse can efficiently adsorb metallic cations present in water bodies (Ajmal et al., 1998; Gurgel et al., 2008a; Karnitz et al., 2009; Naiya et al., 2009) and effluents making this strategy of adsorption very interesting from an economic and environmental point of view (Pereira et al., 2009, 2010). Nowadays, sugarcane bagasse generated after the crushing of sugarcane, is burned to produce steam for the generation of electric energy at sugar and ethanol plants.

Chromium is present in the earth's crust at an average concentration of 10 mg/kg and in the ores it may reach up to more than 50% in weight. After processing of the ore, the metal can be converted to several compounds and used in many industrial processes such as the production of alloys, electrolytic plating, refractory bricks, pigments and tannic agents for leather. Toxic chromium compounds occur naturally at low concentrations in the earth's crust and it is through industrial activities such as fabrication of cement, electroplating, foundries, welding, mining, industrial and municipal waste, incineration, fertilizers, and specially in its use in tanneries that contamination can occur at higher levels (Gurgel et al., 2009). In this context, an alternative use for sugarcane bagasse is described, in principle, as very promising in the removal of heavy metal ions such as Cr^{3+} from contaminated waters and effluents. However, even after solving the problem of water contamination, the disposal of adsorbent materials contaminated with metal ions after the adsorption process does not have an obvious solution nor a specific destination and/or subsequent use, which could therefore make this process economically unfeasible.

Solid materials containing transition metals such as chromium and cobalt are widely used as heterogeneous catalysts in various reactions of interest for chemical, petrochemical, pharmaceutical and food industries (Boor, 1979; Keii, 2004; Robles-Dutenhefner et al., 2004, 2011). An example is the functionalization of monoterpenes to obtain compounds of interest to the fine chemicals industry as well as other substances categorized as essential oils (Robles-Dutenhefner et al., 2009; Sales et al., 2003).

Terpenes constitute a class of natural products that can be transformed into compounds commercially important for industrial production of fragrances, perfumes and flavors (Pybus and Sell, 1999). The application of cobalt and chromium as catalysts for homogeneous and heterogeneous oxidation of terpenes was already reported in the literature by various research groups (da Silva et al., 2003; Robles-Dutenhefner et al., 2004, 2005; Rocha et al., 2009; Speziali et al., 2005, 2009).

Thus, this study aims to develop a process that uses agricultural by-products such as sugarcane bagasse, modified with organic ligands such as succinic anhydride and EDTA dianhydride, and use the adsorbent materials produced to remove Co^{2+} and Cr^{3+} from single metal ion aqueous solutions. Finally, the application of these adsorbent materials containing adsorbed Co^{2+} and Cr^{3+} as heterogeneous catalysts for the chemical transformation of natural terpenic substrates in valuable oxygenated derivatives is presented.

2. Experimental

2.1. Chemicals

Succinic anhydride and pyridine were purchased from Vetec (Brazil). EDTA (disodium salt), acetic anhydride, and N,N'-dimethylformamide (DMF) were purchased from Synth (Brazil). The monoterpenes (β)-citronellol (**1**), (+)-limonene (**2**), (−)-β-pinene (**3**) were purchased from Sigma-Aldrich. Pyridine was refluxed overnight with NaOH and distilled prior to use. DMF was treated with molecular sieve (4 Å) prior to use. $CoCl_2 \cdot 6H_2O$ and $CrCl_3 \cdot 6H_2O$ were purchased from Merck.

2.2. Preparation of the catalysts SCB2-Co and SCB2-Cr from succinylated sugarcane bagasse

The chemical modification of sugarcane bagasse (B) was performed according to the synthetic route shown in Fig. 1. To this end, sugarcane bagasse was initially milled using a tungsten ring mill and sieved using a sieve system composed by screens of 1.68, 0.251, 0.152, and 0.075 mm. Subsequently, the fraction of 0.075 mm was washed with hexane:ethanol 1:1 (v/v) in a Soxhlet apparatus for 24 h and dried in an oven at 80 °C. Sugarcane bagasse (3 g), dry powder (0.075 mm), succinic anhydride (9 g), and anhydrous pyridine (30 mL) were added to a round-bottom flask equipped with a reflux condenser. The suspension was heated at pyridine reflux for 24 h. At the end of the reaction, the succinylated sugarcane bagasse (SCB1) was transferred to a sintered glass funnel with porosity 4 and successively washed with 1.0 mol/L of acetic acid in dichloromethane, 95% ethanol, 0.01 mol/L hydrochloridric acid solution, distilled water, 95% ethanol and then with acetone. SCB1 was dried at 80 °C in an oven for 2 h. Next, SCB1 was cooled in a desiccator and weighed (Gurgel et al., 2008a).

SCB1 was treated with a saturated sodium bicarbonate solution in order to release the carboxylate groups, producing the sorbent material SCB2. Then, SCB2 was washed with distilled water, 95% ethanol, acetone, and dried at 80 °C in an oven for 2 h. After that, SCB2 was separately treated with aqueous spiked solutions of Co^{2+} (0.2 mol/L) and Cr^{3+} (0.2 mol/L) for 1 h, and the solid and liquid fractions were separated using a sintered glass funnel with porosity 4, washed with distilled water, and dried at 80 °C in an oven for 2 h. SCB2 treated with Co^{2+} and Cr^{3+} aqueous solutions was referred to as SCB2-Co and SCB2-Cr, respectively, as can be seen in Fig. 1.

2.3. Preparation of the catalysts EB-Co and EB-Cr from sugarcane bagasse modified with EDTA dianhydride (EDTAD)

The chemical modification of sugarcane bagasse (B) with EDTA dianhydride was carried out using the synthetic route shown in Fig. 2. Sugarcane bagasse (3 g), dry powder (0.075 mm), EDTA dianhydride (15 g), and anhydrous N,N'-dimethylformamide (DMF) (126 mL) were added to a round-bottom flask equipped with a reflux condenser. The mixture was heated at 75 °C under constant magnetic stirring for 24 h. At the end of the reaction, sugarcane bagasse modified with EDTA (EB) was transferred to a sintered glass funnel with porosity 4 and washed with DMF, 95% ethanol, distilled water, saturated sodium bicarbonate solution, distilled water, 95% ethanol, and then with acetone. EB was dried at 80 °C in an oven for 2 h, and then cooled in a desiccator and weighed (Karnitz et al., 2009). After that, EB was subsequently treated with aqueous spiked solutions of Co^{2+} (0.2 mol/L) and Cr^{3+} (0.2 mol/L) for 1 h, and then solid and liquid fractions were separated as described in Section 2.2. EB treated with Co^{2+} and Cr^{3+} aqueous solutions was referred to as EB-Co and EB-Cr, respectively (Fig. 2).

2.4. Biobased catalysts characterization

2.4.1. Fourier transform infrared spectroscopy (FTIR)

Sugarcane bagasse (B), succinylated sugarcane bagasse (SCB1) and modified bagasse with EDTA dianhydride (EB) were characterized by FTIR spectroscopy. Infrared spectra were recorded on a Nicolet Impact 410 FTIR spectrometer by using KBr disk from 4000 to 400 cm^{-1} with 32 scans and 4 cm^{-1} of resolution. The samples were prepared by mixing 1 mg of previous dried B, SCB1, and/or EB with 100 mg of spectroscopic grade KBr powder.

2.4.2. Specific surface area and pore size distribution

The specific surface area (BET method) of SCB2 and EB was measured by the N$_2$ adsorption/desorption isotherms at liquid
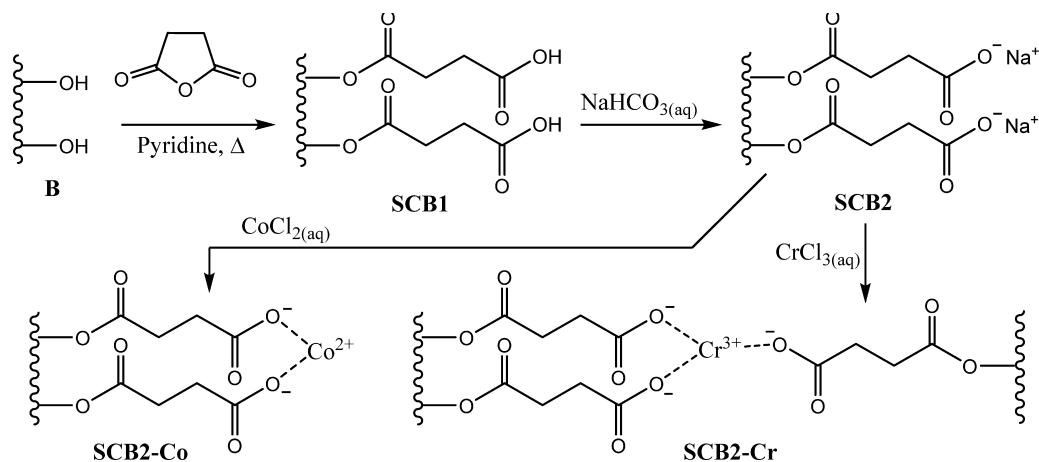
Fig. 1. Synthetic route used to prepare the catalysts SCB2-Co and SCB2-Cr.

nitrogen temperature (77 K) on an Autosorb-Quantachromium (NOVA-1200). The pore size distributions were calculated from the desorption isotherms using the Barrett–Joyner–Halenda (BJH) method.

2.4.3. X-ray diffraction

X-ray diffraction (XRD) patterns of adsorbents containing adsorbed Co^{2+} and Cr^{3+} (SCB2-Co, EB-Co, SCB2-Cr and EB-Cr) were recorded on a Shimadzu diffractometer model XRP-6000 using Mg-filtered Fe K$_\alpha$ radiation (λ = 1.9374 Å) generated at a voltage of 40 kV and current of 30 mA with a scan rate of 2°/min from 7° to 70°.

2.4.4. Thermogravimetric analysis

Thermogravimetry analyses (TGA) of catalysts were carried out in a simultaneous TGA-DTA equipment model SDT 2960 (TA Instruments). The samples were heated from 25 to 900 °C at a linear heating rate of 10 °C/min under synthetic air atmosphere at a flow rate of 50 mL/min.

2.4.5. Co^{2+} and Cr^{3+} contents in the adsorbents

The amount of Co^{2+} and Cr^{3+} adsorbed on SCB2 and EB was determined using inductively coupled plasma atomic emission spectrometry (ICP-AES Spectro model Ciros CDD). For this, a sample of 0.2500 g of catalyst was accurately weighed and transferred
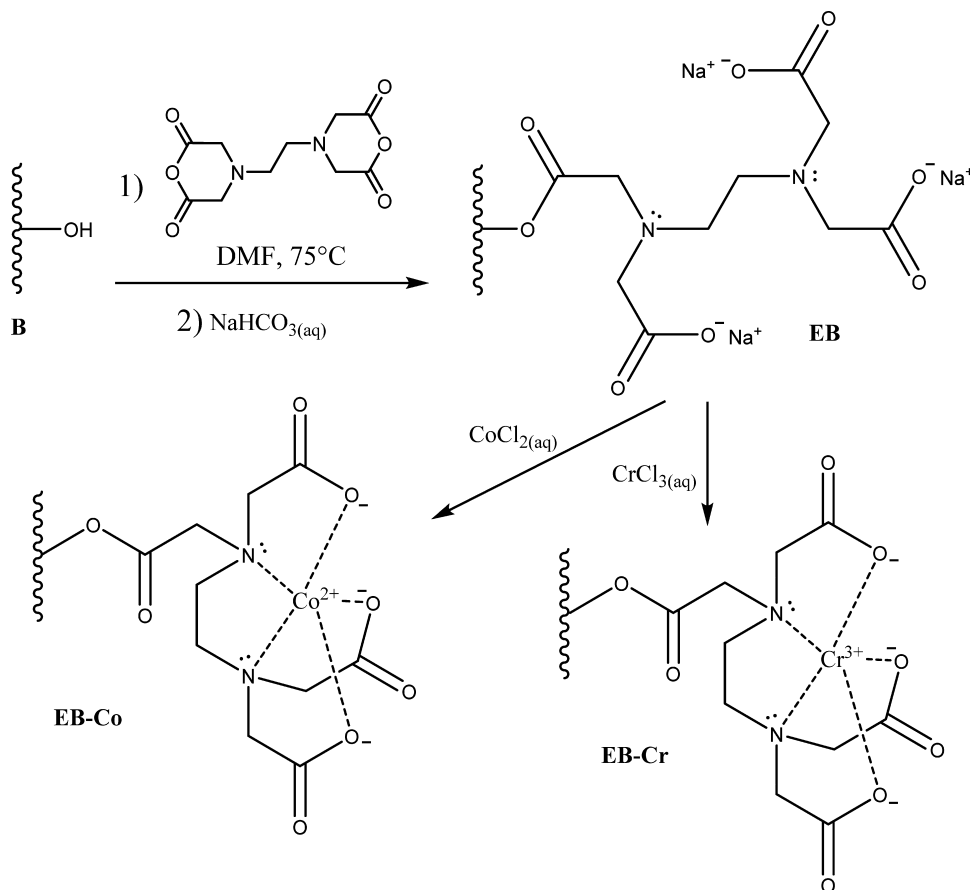

Fig. 2. Synthetic route used to prepare the catalysts EB-Co and EB-Cr.

to a 250 mL Erlenmeyer flask. After that, 10.0 mL of hydrochloric acid/nitric acid aqueous solution, 3:1 (v:v), prepared from concentrated acids were added. The suspension was transferred to a hot plate and heated to 80 °C and kept in this temperature for 15 min. The suspension was cooled and the solid and liquid fractions were separated by single filtration. The concentration of Co^{2+} and Cr^{3+} was determined by ICP-AES.

2.5. Adsorption study of Co^{2+} and Cr^{3+} on SCB2 and EB

The adsorption studies of Co^{2+} and Cr^{3+} on SCB2 and EB were divided into three steps: (1) adsorption as a function of contact time; (2) adsorption as a function of pH of the metal ion solution; and (3) effect of initial metal ion concentration on adsorption.

2.5.1. Adsorption study of Co^{2+} and Cr^{3+} as a function of contact time

Adsorption experiments of Co^{2+} and Cr^{3+} on SCB2 and EB were performed for the purpose of determining the adsorption equilibrium time. 100 mg samples of SCB2 and/or EB were accurately weighed and transferred to 250-mL Erlenmeyer flasks with a 100.0 mL of aqueous Co^{2+} and/or Cr^{3+} solutions of known concentration (190 mg/L for Co^{2+} and 180 mg/L for Cr^{3+}). The Erlenmeyer flasks were mechanically stirred for different periods of time on a rotary shaker at 100 rpm at 25 °C. The pH of the suspensions was adjusted by adding a few drops of aqueous NaOH and/or HCl solutions (0.1–5.0 mol/L) in order to achieve values of 6.4 and 6.0 for adsorption of Co^{2+} on SCB2 and EB and 3.7 and 3.2 for adsorption of Cr^{3+} on SCB2 and EB. At the end of each period of time, adsorbate and adsorbent were separated by single filtration using Whatman-41 quantitative filter paper for instrumental analysis. Three aliquots of 10.0 mL of each metal ion solution were used to determine metal ion equilibrium concentration. Co^{2+} equilibrium concentration was determined by direct titration with aqueous EDTA standard solution (3 mmol/L) at pH 10 using murexide as an indicator and Cr^{3+} equilibrium concentration was determined by back titration of an excess of aqueous EDTA standard solution (3 mmol/L) with aqueous Mg^{2+} standard solution (2 mmol/L) at pH 10 using Eriochrome Black T as an indicator. A buffer solution comprised of NH_3/NH_4^+ was used to adjust the pH to 10 in the both titrations (Gurgel et al., 2008b).

2.5.2. Adsorption study of Co^{2+} and Cr^{3+} as a function of pH

Adsorption experiments of Co^{2+} and Cr^{3+} on SCB2 and EB were carried out to determine the effect of pH on the metal ion adsorption process. Samples of 100 mg were accurately weighed and transferred to 250-mL Erlenmeyer flasks with 100.0 mL of aqueous Co^{2+} and/or Cr^{3+} solutions of known concentration (190 mg/L for Co^{2+} and 180 mg/L for Cr^{3+}). The Erlenmeyer flasks were mechanically stirred for 30 min on a rotary shaker at 100 rpm at 25 °C. The contact time used in this study was that obtained from study of adsorption as a function of contact time (Section 2.5.1). The pH of the suspensions was adjusted by adding a few drops of aqueous NaOH and/or HCl solutions (0.1–5.0 mol/L). The pH range used in the studies was from 2.4 to 7.1 for SCB2-Co, from 1.2 to 6.6 for EB-Co, from 2.0 to 4.5 for SCB2-Cr, and from 2.0 to 4.6 for EB-Cr. Throughout the experiments the pH was checked, and if any variation took place, the pH was corrected to the initial value chosen for each set of experiments. The metal ion equilibrium concentration was determined as described in Section 2.5.1.

2.5.3. Adsorption study of Co^{2+} and Cr^{3+} as a function initial metal ion concentration–adsorption isotherms

Adsorption experiments of Co^{2+} and Cr^{3+} on SCB2 and EB were performed to determine the effect of initial metal ion concentration and to obtain the adsorption isotherms. Samples of 100 mg were

accurately weighed and transferred to 250-mL Erlenmeyer flasks with 100.0 mL of aqueous Co^{2+} and/or Cr^{3+} solutions of known concentration from 120 to 290 mg/L and from 130 to 290 mg/L for Co^{2+} and SCB2/EB adsorbent materials, and from 105 to 280 mg/L for Cr^{3+} and SCB2/EB adsorbent materials, respectively. An equilibrium time of 30 min was chosen for all adsorption systems based on the study of adsorption as a function of contact time. The pH of suspensions of SCB2-Co, SCB2-Cr, EB-Co, and EB-Cr was adjusted for 6.5, 5.8, 5.9, and 4.5, respectively. Some variations of the pH of suspensions were corrected along the time by adding drops of aqueous NaOH and/or HCl solutions (0.1–1 mol/L). The equilibrium concentration of Co^{2+} and Cr^{3+} was also determined by titration as described in Section 2.5.1. Equilibrium adsorption capacities were calculated as follows:

$$q_e = \frac{(C_i - C_e) \times V_m}{m_{ads}} \tag{1}$$

where q_e (mg/g) is the equilibrium adsorption capacity, C_i and C_e (mg/L) initial and equilibrium metal ion concentration, V_m (L) the volume of the metal ion solution, and m_{ads} (g) the mass of adsorbent material.

2.6. Free energy of adsorption

According to Liu (2009), the Gibbs free energy change ($\Delta G°$) indicates the degree of spontaneity of an adsorption process. The $\Delta G°$ of adsorption is calculated as follows:

$$\Delta G° = -RT \ln K_a \tag{2}$$

where R is the gas constant 8.314 J/K mol, T (K) the absolute temperature, and K_a is the thermodynamic equilibrium constant without units. The Langmuir equilibrium constant has been often used for calculation of $\Delta G°$ using Eq. (2) in adsorption studies (Liu, 2009). However, it should be pointed out that the thermodynamic equilibrium constant in Eq. (2) is unitless, whilst the Langmuir constant has units of L/mol. Liu (2009) has demonstrated in detail that the relationship between the Langmuir equilibrium constant, K_L, and the thermodynamic equilibrium constant, K_a, can be given by the following equation.

$$K_a = \left[\frac{K_L}{\gamma_e} \times (1 \quad mol/L) \right] \tag{3}$$

where γ_e is a function of the ionic strength (I_e) ($\log \gamma_e = -Az^2 I_e^{1/2}$) of the solute at adsorption equilibrium and the charge carried by the solute (z) (Debye–Hückel law). According to Liu (2009), in the case of neutral adsorbates, adsorbates with weak charges or for a dilute solution of charged adsorbate, the thermodynamic equilibrium constant of adsorption can be reasonably approximated by the Langmuir equilibrium constant. In this case, the Langmuir equilibrium constant can be applied for determination of $\Delta G°$, and Eq. (3) turns to:

$$\Delta G° \approx -RT \ln \left[K_L \times (1 \, mol/L) \right] = -RT \ln K_L \tag{4}$$

A detailed reading of Liu's discussion is strongly recommended by authors to avoid erroneous use of this approach in the calculation of $\Delta G°$.

2.7. Catalytic evaluation of adsorbent materials

In catalytic oxidation experiments, monoterpenes β-citronellol (**1**), (+)-limonene (**2**), and (−)-β-pinene (**3**) were used. Reactions were carried out in a glass reactor equipped with a magnetic stirrer. The glass reactor was connected to a gas buret containing molecular oxygen to measure the gas uptake. In a typical run, a mixture of β-citronellol (14 mmol), dodecane (4.4 mmol) and the catalyst (0.1 g,
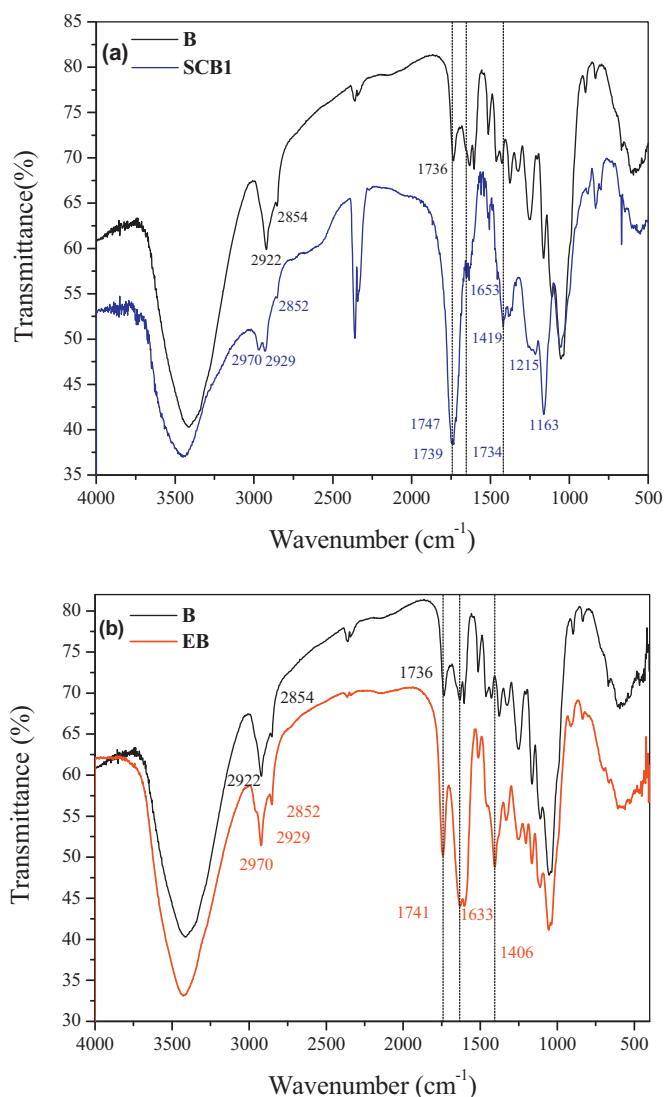
Table 1
Textural properties of SCB2 and EB materials.

Material	BET surface area (m²/g)	Total pore volume (cm³ g⁻¹)	Average pore diameter (Å)
SCB2	2.7	10.0	155.0
EB	1.5	4.0	108.0

hydroxyl groups present in the polysaccharide fraction of sugarcane bagasse. In Fig. 3a, it is noteworthy that functionalization of sugarcane bagasse surface is evidenced by the appearance of bands 2970, 2929, and 2852 cm⁻¹, corresponding to asymmetric and symmetric stretching of the methylene groups (γCH_2) present in succinyl group (Gurgel et al., 2008a). The bands at 1419 and 1215 cm⁻¹ are related to out of plane bending vibrations for the carboxylic acid hydroxyl groups (δOH). Bands 1653 and 1655 cm⁻¹ correspond to carbonyl groups stretching ($\gamma C=O$) also present in the succinyl group. In Fig. 3b, it should be mentioned that in the comparative spectra of B and EB, the appearance of the strong bands at 1743 cm⁻¹ are attributed to axial deformation of ester groups (−O−C=O) and the peak observed at 1631 cm⁻¹ is attributed to axial symmetric deformation of carboxylate groups, both present in the molecule of EDTA which is chemically bonded to sugarcane bagasse. These bands confirm the introduction of EDTA dianhydride in the solid support with consequent release of carboxylate groups (Karnitz et al., 2009).

Table 1 summarizes the textural properties of SCB2 and EB before adsorption experiments. Their BET surface areas are very small with large total pore volume values indicating that functionalization of the sugarcane matrix for the adsorption experiments was effective. Moreover, it also suggests that a chemisorption phenomenon may be occur between the organic matrix and the selected metallic ions.

X-ray diffraction patterns for SCB2-Co, EB-Co, SCB2-Cr, and EB-Cr (figure not shown) indicate that the crystalline structure of cellulose I was maintained after chemical modification of sugarcane bagasse with succinic anhydride and EDTA dianhydride. In addition, no diffraction peaks characteristic for chromium and cobalt phases were noticed in the diffractograms.

Thermogravimetric curves for SCB2-Co, EB-Co, SCB2-Cr, and EB-Cr are shown in Supplementary Fig. 1. As can be seen in Supplementary Fig. 1a–d and in Table 2, the initial small weight loss, which occurred at temperatures between 49 and 60 °C, representing approximately 10–14% of the total weight loss was attributed to the vaporization of bound water in the samples. For all samples, the initial weight loss was followed by a plateau that extended to the start of the main decomposition events and causing weight losses around 70–83%. According to Ouajai and Shanks (2005) and Bilba and Ouensanga (1996) depolymerization, deacetylation and dehydration of hemicelluloses and dehydration and break of

Fig. 3. Comparative FTIR spectra of (a) B and SCB1 and (b) B and EB.

ca. 6.5–12 wt.%) was intensively stirred at 80 °C and oxygen pressure of 1 atm. The reactions were followed by measuring the uptake of oxygen and by gas chromatography (GC) using dodecane as an internal standard (Shimadzu 2014 instrument, Carbowax 20 M capillary column, FID detector). The reactors were placed in an oil bath; then, the solutions were intensively stirred at 60 °C for the reported time. Structures of products were confirmed by gas chromatography coupled to mass spectrometry (Shimadzu QP5000 instrument, DB5 capillary column, 70 eV). Upon completion of the reaction, the catalyst was filtered off, washed with distilled water, EtOH, and reused. To control metal leaching, the catalyst was removed at the reaction temperature after 2 h and the solution was allowed to react further.

3. Results and discussion

3.1. Biobased catalysts characterization

Fig. 3a and b shows FTIR spectra for raw sugarcane bagasse (B), succinylated bagasse (SCB1) and sugarcane bagasse modified with EDTA dianhydride (EB). As can be seen in Fig. 3a and b, the comparative FTIR spectra of both materials show a broad and intense band at 3440 cm⁻¹ assigned to the vibrational (ν_{OH}) modes of the

Table 2
Thermogravimetric data for thermal decomposition of SCB2-Co, SCB2-Cr, EB-Co, and EB-Cr.

	Raw sugarcane bagasse	SCB2-Co	SCB2-Cr	EB-Co	EB-Cr
$T_{D,1}$ (°C)	70	55	53	60	49
ΔM_1 (%)	6.3	14	10	12	10
$T_{D,2}$ (°C)	320	324	318	310	284
$T_{D,3}$ (°C)	376	366	349	349	334
$T_{D,4}$ (°C)	–	392	366	371	359
$\Delta M_{2,3,4}$ (%)	83	70	79	80	83
Residue (M_xO_y, %)	10.7	16	11	8	7
Co (%)[a]	–	12.6	–	6.3	–
Cr (%)[a]	–	–	7.5	–	4.8

[a] In the calculation of the percentages of Co and Cr on SCB2 and EB the formation of CoO and Cr_2O_3 was considered.

α- and β-aryl-alkyl-ether bonds in lignin occurred at about 320 °C. As can be seen in Table 2, the second decomposition temperature ($T_{D,2}$) for the samples SCB2-Co, EB-Co, and EB-Cr is closer to 320 °C, which is in good agreement with the observation made by Ouajai and Shanks (2005) and Bilba and Ouensanga (1996). Ouajai and Shanks (2005) and Bilba and Ouensanga (1996) also noticed that the decomposition event around ~376 °C, third and fourth decomposition events ($T_{D,3}$ and $T_{D,4}$) could be attributed to cellulose decomposition and breaking of C—C bonds between structural units of lignin. This would allow for the decarbonylation and decarboxylation reactions to take place and result in large weight losses.

Supplementary data associated with this article can be found, in the online version, at http://dx.doi.org/10.1016/j.indcrop.2013.07.047.

Chromium and cobalt contents in SCB2-Cr, EB-Cr, SCB2-Co, and EB-Co were quantified by ICP-AES after acidic digestion of catalysts to give values of 6.5%, 5%, 12%, and 9 wt%, respectively. These values may vary according to the adsorption experiment performed. This study aims mainly to assess the reactivity of the material after the adsorption experiment. The influence of optimization of the adsorption process on the catalytic activity of material was not studied in this investigation, but instead, the feasibility of obtaining promising new applications for adsorbents containing metal ions was the main focus here.

3.2. Adsorption study of Co^{2+} and Cr^{3+} on SCB2 and EB

3.2.1. Effect of contact time

Experiments to investigate the effect of contact time on adsorption of Co^{2+} and Cr^{3+} on SCB2 and EB were carried out to determine the adsorption equilibrium time (t_e). As can be seen in Fig. 4a, t_e was attained after 5 min for both metal ions and adsorbent materials. Therefore, a contact time of 30 min was used for the adsorption studies as a function of pH. This time is enough to handle those pH variations that inevitably occur and corrections were made to ensure that initial pH was similar to end pH.

3.2.2. Effect of pH

One of the most important parameters that directly affect the adsorption of Co^{2+} and Cr^{3+} is the pH. The dependence of metal ions uptake on pH is related to pK_a of the functional groups on the surface of the adsorbent material and the form of the metal ion in the solution, i.e. presence of the species such as M^{n+}, $M(OH)^{(n-1)+}$, and $M(OH)_n$. Solubility product constants (Lide, 2012) (Ksp) for Co^{2+} (5.92×10^{-15}) and Cr^{3+} (3.0×10^{-29}) were used to calculate the maximum pH at which these metal ions may not occur as hydrolyzed species. Based on Co^{2+} and Cr^{3+} concentrations and their Ksp, the maximum pH values that can be used for adsorption studies were found to be 8.1 and 5.3, respectively. SCB2 is expected to be a weakly basic ion exchanger, while EB is an amphoteric and contains both acidic and basic functional groups as can be seen in Figs. 1 and 2. As can be seen in Fig. 4b, at pH lower than 3.5, functional groups of SCB2 are essentially protonated and the adsorption capacity (q) of Co^{2+} and Cr^{3+} is very low at this pH. Increasing the pH, the carboxylic acid groups are deprotonated and the adsorption capacity consequently increased and reached a plateau for SCB-Co^{2+}. For the adsorption system SCB-Cr^{3+}, increasing pH increased the adsorption capacity, however no plateau was noticed due to restriction of the maximum pH for Cr^{3+} adsorption. As can be seen in Fig. 4b, at low pH 1–2, functional groups of EB are partially protonated and the adsorption capacity (q) of Co^{2+} and Cr^{3+} is low, but larger than for SCB2 at the same pH range. Increasing the pH, the adsorption capacity is also increased. For Co^{2+}, q increases as pH was increased and reached a plateau, while for Cr^{3+} q increases as pH was increased, but no plateau was attained. This observation is
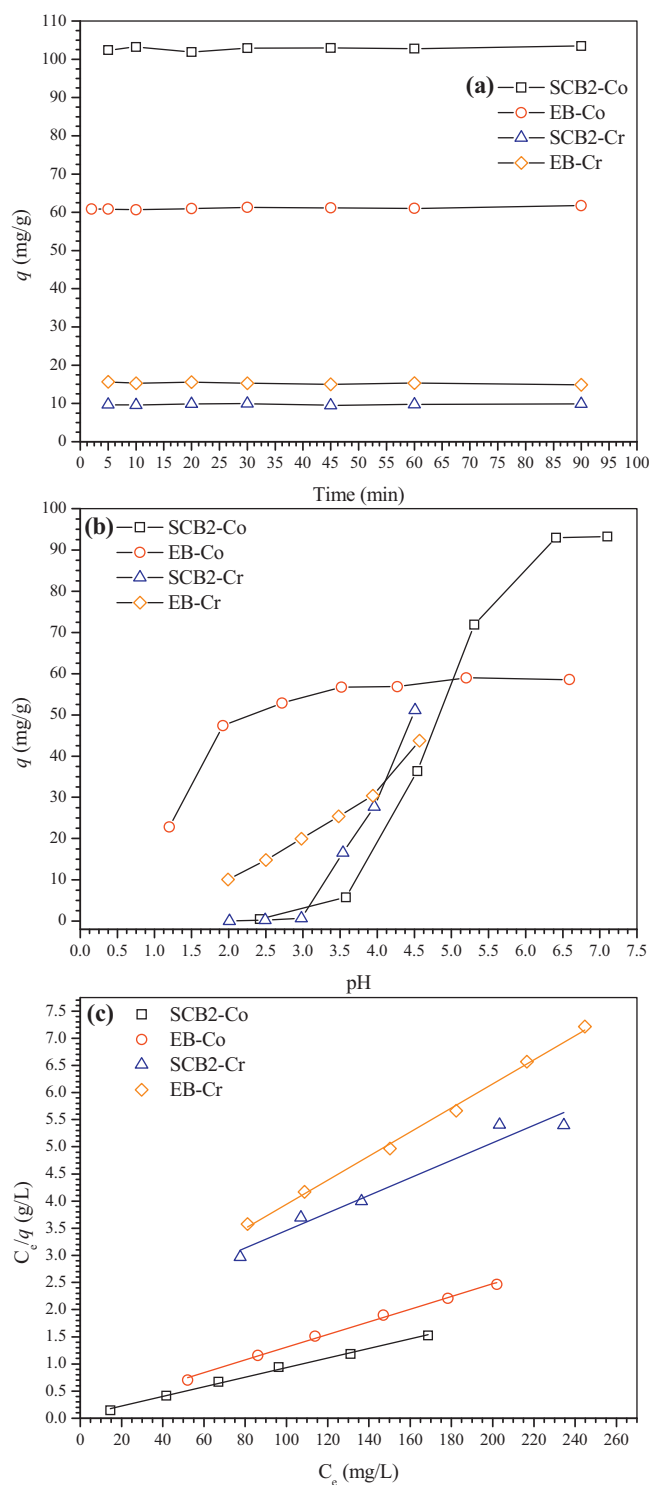

Fig. 4. Studies of adsorption of Co^{2+} and Cr^{3+} on SCB2 and EB: (a) effect of contact time, (b) effect of pH, and (c) effect of initial metal ion concentration–adsorption isotherms.

similar to that noticed for Co^{2+} and Cr^{3+} adsorption on SCB2. The larger adsorption capacity of EB in relation to SCB2 at low pH values is attributed to the chemical properties of iminoacetate groups from EDTA, which have lower pK_a values than succinyl groups. The low pK_a values of the iminoacetate groups make it possible for EB to adsorb metal ions at low pH values, which gives to EB adsorbent material special properties.

Table 3
Langmuir parameters for adsorption of Co^{2+} and Cr^{3+} on SCB2 and EB.

Metal ion	Material	pH	Langmuir adsorption data					
			Q_{max} (mg/g)	Q_{max} (mmol/g)	b (L/mg)	R^2	$-\Delta G°$ (kJ/mol)	SSR
Co^{2+}	SCB2	6.4	113.12 ± 3.32	1.92 ± 0.06	0.184 ± 0.101	0.9957	23.04 ± 1.36	0.004
	EB	5.8	85.69 ± 2.44	1.45 ± 0.04	0.083 ± 0.027	0.9960	21.06 ± 0.82	0.007
Cr^{3+}	SCB2	5.9	61.92 ± 6.90	1.19 ± 0.13	0.009 ± 0.002	0.9522	15.18 ± 0.48	0.167
	EB	4.5	45.09 ± 1.21	0.87 ± 0.02	0.013 ± 0.001	0.9964	16.13 ± 0.16	0.028

3.2.3. Effect of initial metal ion concentration and adsorption isotherms

Adsorption isotherms can be used to describe how adsorbates interact with adsorbents. In this sense, Langmuir adsorption isotherm model has traditionally been used to quantify and contrast the performance of different biosorbent materials. A linearized form of Langmuir equation is shown as follows (Langmuir, 1918):

$$\frac{C_e}{q_e} = \frac{1}{Q_{max}b} + \frac{C_e}{Q_{max}} \qquad (5)$$

where q_e (mg/g) is the equilibrium adsorption capacity, Q_{max} (mg/g) is the maximum amount of metal ion *per* unit weight of SCB2 and/or EB to form a complete monolayer coverage on the surface bound at high equilibrium metal ion concentration, C_e (mg/L) is the equilibrium metal ion concentration, and b (L/mg) is the Langmuir constant related to the affinity of binding sites. Q_{max} characterizes the practical limiting adsorption capacity when the surface is fully covered by metal ions and b represents the bond energy related to the adsorption phenomenon between metal ions and biosorbent materials.

A linearized plot of C_e/q_e against C_e is obtained from the Langmuir model and is shown in Fig. 4c. Q_{max} and b were computed from the slopes and intercepts of different straight lines obtained from linear regression analysis of the experimental data (Fig. 4c). The high coefficients of determination obtained by fitting experimental data with Langmuir model indicate that the adsorption phenomenon of Co^{2+} and Cr^{3+} can be described by this model.

The results for Co^{2+} and Cr^{3+} adsorption on SCB2 and EB using Langmuir model are presented in Table 3. These results are very close to those obtained by ICP-AES. For example, Q_{max} for Co^{2+} adsorption on SCB2 is 113.1 mg/g, corresponding to 11.31 wt% of Co^{2+}, which is coherent with those results obtained by ICP-AES (12 wt%). For all the obtained materials, EB-Cr, EB-Co, SCB2-Cr, and SCB2-Co, the variations between the obtained results from ICP-AES method and adsorption isotherms were in a range from 5 to 10%, and thus confirming the content of Co^{2+} and Cr^{3+} in the adsorbents.

SCB2 exhibited larger maximum adsorption capacity (Q_{max}) and Langmuir constant (b) than EB for Co^{2+} and Cr^{3+} adsorption. Recapitulating, SCB2 showed larger Q_{max} values for Co^{2+} and Cr^{3+} adsorption in pH values closer to 6, however SCB2 exhibited a smaller adsorption capacity (q) than EB in pH values from 1 to 3. Therefore, SCB2 may be used to treat effluents containing metal ions in pH values higher than 3.5–4.0, while EB may be used to treat effluents in more acidic pH values.

The majority of the materials tested for metallic cationic adsorption in the literature do not present a good capacity of adsorption in acidic conditions (Karnitz et al., 2009). In addition, the results obtained in this study showed that there is the possibility of modulating the performance of the adsorbent materials to suite the pH of the aqueous system by specific surface modifications. In acidic pH values, EDTA ligand grafted to bagasse provided good adsorption performance for the adsorbent material EB, while in less acidic pH, succinic anhydride grafted to bagasse provided a larger adsorption capacity for the adsorbent material SCB2. Therefore, mixing both adsorbent materials could be very useful for treating effluents with varying pH ranges and thus affording highly versatile materials.

3.3. Catalytic evaluation

The aim of the present study was to investigate the application of the biosorbents SCB2 and EB as heterogeneous catalysts. These materials were applied in the catalytic oxidation of terpenic substrates as β-citronellol (**1**), (+)-limonene (**2**) and (−)-β-pinene (**3**). Citronellal (**4**) and citronellol epoxide (**5**) are the main products from β-citronellol (**1**) oxidation. The oxidation products of (+)-limonene (**2**) are carveol (**6**), carvona (**7**) and limonene epoxide (**8**). Pinocarveol (**9**), myrtenal (**10**) and myrtenol (**11**) are the oxidation products of (−)-β-pinene (**3**) with neither epoxide nor corresponding glycol derivatives being detected in the reaction medium. The obtained results are shown in detail in Table 4.

The allylic oxidation and epoxidation products were obtained, despite the main mechanism being allylic oxidation according to literature (Sales et al., 2003). In these reactions a free radical chain mechanism is usually suggested a competition between the abstraction of the allylic hydrogen to give allylic oxidation products and the addition of the alkylperoxy radical to the double bond resulting in epoxide products is expected (Sheldon and Kochi, 1981). However, citronellal (**4**) is the main product of citronellol oxidation corresponding to alcohol function oxidation. Furthermore, it is also possible to notice that the chromium ion adsorbed on both materials promoted the highest conversions to citronellal.
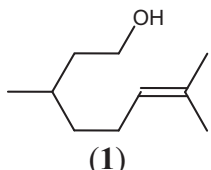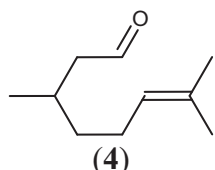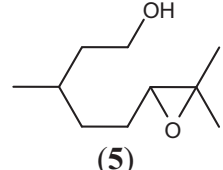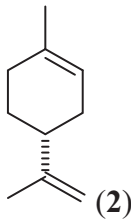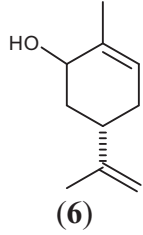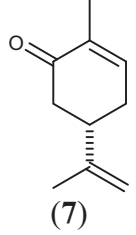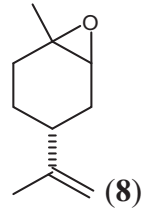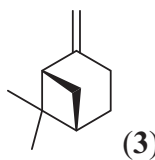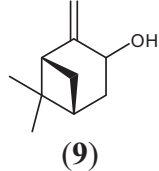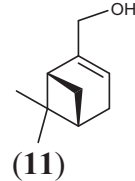
As expected (Robles-Dutenhefner et al., 2009) there is a strong effect of monoterpene structure on the product nature as can be seen in Table 4. (+)-Limonene (**2**) and β-citronellol (**1**) yielded epoxidation products, while the oxidation products of (−)-β-pinene (**3**) were only formed by allylic oxidation, which also occurs with (+)-limonene (**2**).

A blank reaction with all substrates, in which no catalyst was added showed virtually no activity (<10% conversion for 24 h) (these reactions are not shown in the Table 4). The effect of modified matrices containing adsorbed Co^{2+} and Cr^{3+} in succinylated bagasse (SCB2) and sugarcane bagasse modified with EDTA dianhydride (EB) was evaluated.

The results of β-citronellol (**1**), (+)-limonene (**2**) and (−)-β-pinene (**3**) oxidation showed that the catalysts tested were promising for oxidation reactions of the studied monoterpenes, with conversion results ranging between 49 and 78% and with combined selectivity for oxidation products up to 59%. The difference in mass balance (Table 4) was attributed to the formation of oligomers, which were not identified by gas chromatography.

Both chromium and cobalt promoted high conversions and selectivity values in succinylated bagasse matrix (SCB2). The adsorbents containing cobalt were more active than those with chromium (Table 4). The difference in activity between catalysts can be attributed to different oxidative mechanisms between cobalt and chromium. However, the highest *turnover number* (TON) values, which consist in the molar ratio between converted substrate and metal under consideration, were obtained for catalysts in EB as a result of lower metal content adsorbed to this matrix.

Table 4
Oxidation of β-citronellol (**1**), (+)-limonene (**2**) and (−)-β-pinene (**3**) catalyzed by Co and Cr adsorbents under solvent-free conditions.[a]

Substrate	Catalyst	Conversion[b] (%)	Selectivity[b] (%)			TON[c]

(**1**)   (**4**) Oxidation   (**5**) Epoxidation

	SCB2-Cr	58	23		21	125
	EB-Cr	49	19		18	137
	SCB2-Co	67	32		14	104
	EB-Co	61	28		13	108

(**2**)   (**6**)   (**7**)   (**8**)

Allylic oxidation   Epoxidation

	SCB2-Cr	75	15	19	13	180
	EB-Cr	60	12	14	5	185
	SCB2-Co	78	27	22	10	115
	EB-Co	73	21	17	8	143

(**3**)   (**9**)   (**10**)   (**11**)

Allylic oxidation

	SCB2-Cr	70	9	19	21	180
	EB-Cr	58	7	16	19	192
	SCB2-Co	76	9	22	27	119
	EB-Co	69	8	19	22	144

[a] Reaction conditions: 0.100 g of catalyst, 353 K, substrate = 5 mL, O_2 1 atm, and 12 h.
[b] Determined by gas chromatography. The other products were not identified.
[c] TON – mol of substrate/mol of Cr or Co.

A preliminary analysis of differences in results obtained by the studied matrices indicated that SCB2 favors cobalt and chromium metals to promote higher conversions and selectivities than EB. The lower conversion and selectivity results obtained using catalysts in EB can be attributed to the EDTA moiety, which is a polydentate ligand and forms a stable coordination complex with the metal ion. For this reason, only few coordination sites are available for the catalytic process.

In addition, reports on the autoxidation of a number of monoterpenes including α-pinene (Gomes and Antunes, 1997; Lajunen, 2001; Lajunen et al., 2000; Rothenberg et al., 1998), β-pinene (Gomes and Antunes, 1997), and limonene (Gomes and Antunes, 1997) in the presence of cobalt complexes have been previously published. These reports have demonstrated that these substrates yielded complex mixtures of oxygenated derivatives with a very low selectivity for allylic oxidation products. Furthermore, homogeneous and heterogeneous catalytic oxidations of monoterpenes (α-pinene, β-pinene, and limonene) using cobalt as catalyst were also previously studied (Gomes and Antunes, 1997; Lajunen, 2001; Lajunen et al., 2000; Robles-Dutenhefner et al., 2004; Rothenberg et al., 1998). Thus, comparing the results reported above with the results obtained in this study it is possible to notice

that the oxidation of monoterpenes (α-pinene, β-pinene, and limonene) also yielded products from allylic oxidation. However, a higher conversion of the substrates was observed in the present study.

The Co and Cr catalysts can be removed from the reaction mixture by simple centrifugation or filtration and washed after the reaction with a mixture of ethanol/water. The recovered catalysts after washing can be reused several times without a significant loss of activity and selectivity. No significant leaching was observed suggesting a strong interaction between the matrix and the metallic ion, since the adsorption process occurs by complexation of a cation by carboxylate ($-COO^-$) and amino groups ($-NR_1R_2$), resulting in the formation of chelates with high stability. This behavior is very important technologically. Thus, as the catalyst did not release cobalt and chromium to the medium, it can be easily recovered either by centrifugation or filtration and re-used.

The use of biomass-based compounds, chromium and cobalt immobilized on a solid matrix as the catalysts, molecular oxygen as the final oxidant and free solvent conditions are significant practical advantages of this environmentally friendly process and add value to the metal contaminated adsorbents.

4. Conclusions

In this study, an alternative application for adsorbent materials was proposed. To the best of our knowledge, this study is the first case in which lignocellulosic adsorbents are applied in a catalytic oxidation process. The oxidation of β-citronellol(**1**), (+)-limonene(**2**) and (−)-β-pinene(**3**) resulted in highly valuable allylic oxygen derivatives. In addition, the adsorbents may be reused at least three times as catalyst without detectable leaching and significant loss of their activity. Furthermore, the adsorption studies also demonstrated that the adsorbents can be used to treat effluents in a large pH range, which can be very useful in industrial processes.

Acknowledgments

References

Ajmal, M., Khan, A.H., Ahmad, S., Ahmad, A., 1998. Role of sawdust in the removal of copper(II) from industrial wastes. Water Research 32, 3085–3091.

Bilba, K., Ouensanga, A., 1996. Fourier transform infrared spectroscopic study of thermal degradation of sugar cane bagasse. Journal of Analytical and Applied Pyrolysis 38, 61–73.

Boor, J., 1979. Ziegler-Natta Catalysts and Polymerization. Academic Press, New York.

CONAB, 2011. Companhia Nacional de Abastecimento. Avaliação da safra agrícola brasileira de cana-de-açúcar, safra 2011/2012, terceiro levantamento, Dezembro (in Portuguese).

da Silva, M.J., Robles-Dutenhefner, P., Menini, L., Gusevskaya, E.V., 2003. Cobalt catalyzed autoxidation of monoterpenes in acetic acid and acetonitrile solutions. Journal of Molecular Catalysis A: Chemical 201, 71–77.

Gomes, M.d.F.T., Antunes, O.A.C., 1997. Autoxidation of limonene, α-pinene and β-pinene by dioxygen catalyzed by Co(OAc)₂/bromide. Journal of Molecular Catalysis A: Chemical 121, 145–155.

Gurgel, L.V.A., de Freitas, R.P., Gil, L.F., 2008a. Adsorption of Cu(II), Cd(II), and Pb(II) from aqueous single metal solutions by sugarcane bagasse and mercerized sugarcane bagasse chemically modified with succinic anhydride. Carbohydrate Polymers 74, 922–929.

Gurgel, L.V.A., de Melo, J.C.P., de Lena, J.C., Gil, L.F., 2009. Adsorption of chromium (VI) ion from aqueous solution by succinylated mercerized cellulose functionalized with quaternary ammonium groups. Bioresource Technology 100, 3214–3220.

Gurgel, L.V.A., Junior, O.K., Gil, R.P.D.F., Gil, L.F., 2008b. Adsorption of Cu(II), Cd(II), and Pb(II) from aqueous single metal solutions by cellulose and mercerized cellulose chemically modified with succinic anhydride. Bioresource Technology 99, 3077–3083.

Karnitz, O., Gurgel, L.V.A., de Freitas, R.P., Gil, L.F., 2009. Adsorption of Cu(II), Cd(II), and Pb(II) from aqueous single metal solutions by mercerized cellulose and mercerized sugarcane bagasse chemically modified with EDTA dianhydride (EDTAD). Carbohydrate Polymers 77, 643–650.

Karnitz, O., Gurgel, L.V.A., de Melo, J.C.P., Botaro, V.R., Melo, T.M.S., Gil, R.P.D.F., Gil, L.F., 2007. Adsorption of heavy metal ion from aqueous single metal solution by chemically modified sugarcane bagasse. Bioresource Technology 98, 1291–1297.

Keii, T., 2004. Heterogeneous Kinetics. Springer, Berlin.

Lajunen, M.K., 2001. Co(II) catalysed oxidation of α-pinene by molecular oxygen: part III. Journal of Molecular Catalysis A: Chemical 169, 33–40.

Lajunen, M.K., Maunula, T., Koskinen, A.M.P., 2000. Co(II) catalysed oxidation of α-pinene by molecular oxygen. Part 2. Tetrahedron 56, 8167–8171.

Langmuir, I., 1918. The adsorption of gases on plane surfaces of glass, mica and platinum. Journal of the American Chemical Society 40, 1361–1403.

Lide, R.D., 2012. Section 5: Thermochemistry, Electrochemistry, and Kinetics. CRC Handbook of Chemistry and Physics, 92nd ed. CRC Press/Taylor and Francis, Boca Raton, pp. 196–198.

Liu, C.F., Sun, R.C., Qin, M.H., Zhang, A.P., Ren, J.L., Ye, J., Luo, W., Cao, Z.N., 2008. Succinoylation of sugarcane bagasse under ultrasound irradiation. Bioresource Technology 99, 1465–1473.

Liu, C.F., Sun, R.C., Zhang, A.P., Ren, J.L., Wang, X.A., Qin, M.H., Chao, Z.N., Luo, W., 2007. Homogeneous modification of sugarcane bagasse cellulose with succinic anhydride using a ionic liquid as reaction medium. Carbohydrate Research 342, 919–926.

Liu, Y., 2009. Is the free energy change of adsorption correctly calculated? Journal of Chemical and Engineering Data 54, 1981–1985.

Naiya, T.K., Chowdhury, P., Bhattacharya, A.K., Das, S.K., 2009. Saw dust and neem bark as low-cost natural biosorbent for adsorptive removal of Zn(II) and Cd(II) ions from aqueous solutions. Chemical Engineering Journal 148, 68–79.

Ouajai, S., Shanks, R.A., 2005. Composition, structure and thermal degradation of hemp cellulose after chemical treatments. Polymer Degradation and Stability 89, 327–335.

Pereira, F.V., Gurgel, L.V.A., de Aquino, S.F., Gil, L.F., 2009. Removal of Zn(2+) from electroplating wastewater using modified wood sawdust and sugarcane bagasse. Journal of Environmental Engineering-ASCE 135, 341–350.

Pereira, F.V., Gurgel, L.V.A., Gil, L.F., 2010. Removal of Zn(2+) from aqueous single metal solutions and electroplating wastewater with wood sawdust and sugarcane bagasse modified with EDTA dianhydride (EDTAD). Journal of Hazardous Materials 176, 856–863.

Pybus, D.H., Sell, C.S., 1999. The Chemistry of Fragrances (RSC Paperbacks). Royal Society of Chemistry, Cambridge.

Robles-Dutenhefner, P.A., Brandao, B.B.N.S., de Sousa, L.F., Gusevskaya, E.V., 2011. Solvent-free chromium catalyzed aerobic oxidation of biomass-based alkenes as a route to valuable fragrance compounds. Applied Catalysis A: General 399, 172–178.

Robles-Dutenhefner, P.A., da Silva, M.J., Sales, L.S., Sousa, E.M.B., Gusevskaya, E.V., 2004. Solvent-free liquid-phase autoxidation of monoterpenes catalyzed by sol–gel CO/SiO₂. Journal of Molecular Catalysis A: Chemical 217, 139–144.

Robles-Dutenhefner, P.A., Rocha, K.A.D., Sousa, E.M.B., Gusevskaya, E.V., 2009. Cobalt-catalyzed oxidation of terpenes: Co-MCM-41 as an efficient shape-selective heterogeneous catalyst for aerobic oxidation of isolongifolene under solvent-free conditions. Journal of Catalysis 265, 72–79.

Robles-Dutenhefner, P.A., Speziali, M.G., Sousa, E.M.B., dos Santos, E.N., Gusevskaya, E.V., 2005. Selective hydrogenation of myrcene catalyzed by sol–gel Pd/SiO₂. Applied Catalysis A: General 295, 52–58.

Rocha, K.A.D., Robles-Dutenhefner, P.A., Kozhevnikov, I.V., Gusevskaya, E.V., 2009. Phosphotungstic heteropoly acid as efficient heterogeneous catalyst for solvent-free isomerization of alpha-pinene and longifolene. Applied Catalysis A: General 352, 188–192.

Rothenberg, G., Yatziv, Y., Sasson, Y., 1998. Comparative autoxidation of 3-Carene and α-Pinene: factors governing regioselective hydrogen abstraction reactions. Tetrahedron 54, 593–598.

Sales, L.S., Robles-Dutenhefner, P.A., Nunes, D.L., Mohallem, N.D.S., Gusevskaya, E.V., Sousa, E.M.B., 2003. Characterization and catalytic activity studies of sol–gel Co-SiO₂ nanocomposites. Materials Characterization 50, 95–99.

Sheldon, R.A., Kochi, J.K., 1981. Metal-Catalyzed Oxidations of Organic Compounds. Academic Press, London.

Speziali, M.G., Costa, V.V., Robles-Dutenhefner, P.A., Gusevskaya, E.V., 2009. Aerobic palladium(II)/copper(II)-catalyzed oxidation of olefins under chloride-free nonacidic conditions. Organometallics 28, 3186–3192.

Speziali, M.G., Moura, F.C.C., Robles-Dutenhefner, P.A., Araujo, M.H., Gusevskaya, E.V., dos Santos, E.N., 2005. Selective hydrogenation of myrcene catalyzed by complexes of ruthenium, chromium, iridium and rhodium. Journal of Molecular Catalysis A: Chemical 239, 10–14.

Srivastava, V.C., Mall, I.D., Mishra, I.M., 2006. Equilibrium modelling of single and binary adsorption of cadmium and nickel onto bagasse fly ash. Chemical Engineering Journal 117, 79–91.

Sud, D., Mahajan, G., Kaur, M.P., 2008. Agricultural waste material as potential adsorbent for sequestering heavy metal ions from aqueous solutions – a review. Bioresource Technology 99, 6017–6027.

Sun, X.F., Sun, R.C., Tomkinson, J., Baird, M.S., 2003. Preparation of sugarcane bagasse hemicellulosic succinates using NBS as a catalyst. Carbohydrate Polymers 53, 483–495.

Xiao, B., Sun, X.F., Sun, R.C., 2001. The chemical modification of lignins with succinic anhydride in aqueous systems. Polymer Degradation and Stability 71, 223–231.

Yu, J.X., Tong, M., Sun, X.M., Li, B.H., 2008. Enhanced and selective adsorption of Pb²⁺ and Cu²⁺ by EDTAD-modified biomass of baker's yeast. Bioresource Technology 99, 2588–2593.